THE JOURNAL OF BIOLOGICAL CHEMISTRY VOL. 286, NO. 31, pp. 27247–27254, August 5, 2011

Photoprotection in Plants Involves a Change in Lutein 1 Binding Domain in the Major Light-harvesting Complex of Photosystem II*

Received for publication, March 2, 2011, and in revised form, May 13, 2011 Published, JBC Papers in Press, June 6, 2011, DOI 10.1074/jbc.M111.234617

Cristian Ilioaia[‡§1], Matthew P. Johnson[¶], Pen-Nan Liao[‖], Andrew A. Pascal[‡], Rienk van Grondelle[§], Peter J. Walla[‖], Alexander V. Ruban[¶], and Bruno Robert[‡2]**

*From the [‡]Commisariat à l'Energie Atomique, Institut de Biologie et Technologies de Saclay and CNRS URA 2096, F-91191 Gif sur Yvette, France, the [§]Department of Physics and Astronomy, Faculty of Sciences, VU University Amsterdam, De Boelelaan 1081, 1081 HV Amsterdam, The Netherlands, the [¶]School of Biological and Chemical Sciences, Queen Mary University of London, Mile End, Bancroft Road, London E1 4NS, United Kingdom, the [‖]Department of Biophysical Chemistry, Institute of Physical and Theoretical Chemistry, Technische Universität Braunschweig, Hans-Sommer-Strasse 10, 38106 Braunschweig, Germany, and the **Department of Spectroscopy and Photochemical Kinetics, Max Planck Institute for Biophysical Chemistry, Am Fassberg 11, 37077 Göttingen, Germany*

Nonphotochemical quenching (NPQ) is the fundamental process by which plants exposed to high light intensities dissipate the potentially harmful excess energy as heat. Recently, it has been shown that efficient energy dissipation can be induced in the major light-harvesting complexes of photosystem II (LHCII) in the absence of protein-protein interactions. Spectroscopic measurements on these samples (LHCII gels) in the quenched state revealed specific alterations in the absorption and circular dichroism bands assigned to neoxanthin and lutein 1 molecules. In this work, we investigate the changes in conformation of the pigments involved in NPQ using resonance Raman spectroscopy. By selective excitation we show that, as well as the twisting of neoxanthin that has been reported previously, the lutein 1 pigment also undergoes a significant change in conformation when LHCII switches to the energy dissipative state. Selective two-photon excitation of carotenoid (Car) dark states (Car S_1) performed on LHCII gels shows that the extent of electronic interactions between Car S_1 and chlorophyll states correlates linearly with chlorophyll fluorescence quenching, as observed previously for isolated LHCII (aggregated *versus* trimeric) and whole plants (with *versus* without NPQ).

The photosynthetic process starts with the absorption of incoming solar photons by specialized pigment-protein complexes. In plants, light energy is absorbed by the two multisubunit protein-cofactor complexes, photosystem I (PSI)[3] and photosystem II (PSII), and the excitation energy is efficiently transferred to their reaction centers where photochemistry takes place. When these organisms are in low light environments, the process of light energy collection is extremely efficient. However, this process is regulated when the incoming light energy is above that which can be used in electron transport. In these latter conditions, the light-harvesting antenna is able to switch into a photoprotective mode, dissipating the excess energy as heat (1–3). This regulatory mechanism is measured as nonphotochemical quenching of chlorophyll (Chl) fluorescence (NPQ). In higher plants NPQ is a multicomponent process whose major component is called qE (energy-dependent quenching) (4), dependent upon the formation of the proton gradient (ΔpH) across the thylakoid membrane (which itself results from photosynthetic activity) (5). qE is facilitated by the deepoxidation of violaxanthin to zeaxanthin in the xanthophyll cycle (6). The PsbS protein also plays a crucial role in this process, possibly acting as a pH sensor (7, 8). A key characteristic of the qE process is that it is induced in seconds and thus cannot involve *de novo* protein synthesis, but rather corresponds to a reorganization of the existing photosynthetic architecture.

In the past decade a large amount of work has been performed to gain insight in the molecular mechanism(s) underlying this process, and several hypotheses have been put forward (9–12). Among these, it was in particular proposed that excitation energy quenching during qE involves charge transfer and would result from the formation of a carotenoid (Car) cation/Chl anion pair, which dissipates the excitation energy upon recombination to the ground state (10, 11, 13). Formation of a radical cation was reported in the reconstituted minor antenna complexes as well as in thylakoid membranes, but not in puri-

* This work was supported by The Netherlands Organization for Scientific Research via the Foundation of Earth and Life Sciences (to C. I. and R. v. G.), the European Union FP7 Marie Curie Reintegration Grant ERG 224796 (to C. I.), research and equipment grants from the United Kingdom Biotechnology and Biological Sciences Research Council and Engineering and Physical Sciences Research Council (to A. V. R. and M. P. J.), the German Science Foundation (to P.-N. L. and P. J. W.), Blaise Pascal Chair from the Fondation of the Ecole Normale Supérieure (to R. v. G.), a European Union FP7 Marie Curie HARVEST Network grant and European Research Council Grant PhotProt (to B. R. and R. v. G.).

[1] To whom correspondence may be addressed: Dept. of Physics and Astronomy, Faculty of Sciences, VU University Amsterdam, De Boelelaan 1081, 1081 HV Amsterdam, The Netherlands. Tel.: 31-205987935; E-mail: cristian.ilioaia@cea.fr.

[2] To whom correspondence may be addressed. Tel.: 33-169089015; Fax: 33-169088717; E-mail: bruno.robert@cea.fr.

[3] The abbreviations used are: PSI, photosystem I; PSII, photosystem II; Car, carotenoid; Car S_1, Car S_1 (dark) state; Chl, chlorophyll; ΔpH, proton gradient across the thylakoid membrane; k_d, quenching constant used to define quenching of LHCII gel samples; LHCII, light harvesting antenna complex of photosystem II; Lut1, lutein 1 Car bound to LHCII; Neo, neoxanthin Car bound to LHCII; NPQ, nonphotochemical Chl fluorescence quenching; qE, rapidly reversible component of NPQ.

TABLE 1

Pigment composition of isolated LHCII

Trimeric LHCII was prepared from WT and *npq2 Arabidopsis* plants (see "Experimental Procedures"). Data are mmol of Car/mol of Chl *a* + *b*, expressed as means ± S.E. from four replicates. Values in parentheses represent the Car content per monomer of protein (molar ratio), considering that one monomer has 14 Chls (8 Chl *a* and 6 Chl *b* (as in ref. 33). Vio, violaxanthin; Ant, antheraxanthin; Lut, lutein; Zea, zeaxanthin; Neo, neoxanthin.

LHCII	Neo	Vio	Ant	Lut	Zea	Car/ Chl	Chl *a*/*b*
WT	61 ± 1.1 (0.89 ± 0.01)	12 ± 1.6 (0.18 ± 0.02)	0	132 ± 2.6 (1.97 ± 0.03)	0	0.22	1.35 ± 0.1
npq2	0	0	0	131 ± 4.2 (1.87 ± 0.05)	45 ± 6.6 (0.65 ± 0.09)	0.18	1.35 ± 0.1

fied LHCII complexes, suggesting that the former proteins house the quenching site(s). However, other results suggest that this is not the case and that the quenching site is in LHCII. For instance, Bode *et al*. have observed a direct correlation between electronic Car S_1-Chl interactions and quenching properties in both isolated LHCII and entire plants. The linear correlation observed between the Car S_1-Chl *a* interactions in LHCII with NPQ indicates that the Car S_1 state is involved in qE and, according to these results, the quenching results from a short lived Car-Chl excited state (9, 14). Recently, Holzwarth *et al*. have suggested that Cars are not directly involved in qE (15); rather, they propose that quenching in LHCII aggregates involves the formation of a Chl-Chl charge transfer state, characterized by weak far-red fluorescence emission (16). It was further proposed that qE may involve both quenching in LHCII aggregates and also at a separate site involving the PSII core and minor antenna complexes (12).

We originally proposed that trimeric LHCII is the site of qE (9, 17, 18) and that the formation of the quenching site involves a conformational change within this complex. Indeed, reversible fluorescence red shifts (up to 75 nm) have recently been observed in single trimeric LHCII complexes and were explained in terms of specific conformational dynamics of the protein scaffold (19). The conformational change is revealed by resonance Raman spectroscopy, a powerful and selective vibrational technique that gives access to the fine structure of photosynthetic chromophores. These conformational changes involve an alteration in Chl-protein interactions as well as in the planarity of the LHCII-bound neoxanthin (Neo) carotenoid. In isolated LHCII, the amplitude of the signal revealing this Neo structural change correlates linearly with the extent of quenching (9). Furthermore, the same signal was observed in intact chloroplasts and leaves after NPQ induction, and the correlation with the extent of quenching was maintained in these *in vivo* samples. The formation of NPQ is also associated with certain absorption changes that have been suggested to reflect a conformational change in LHCII, brought about by its protonation. The light − dark recovery absorption difference spectrum is characterized by a series of positive and negative bands, the best-known of which is ΔA535 (20). Using resonance Raman the origin of ΔA535 was shown to be a sub-population of red-shifted zeaxanthin molecules (21). In the absence of zeaxanthin (and antheraxanthin) a proportion of NPQ remains and the ΔA535 change is blue-shifted to 525 nm (ΔA525) (22). Using the Raman technique we have shown recently that the ΔA525 absorption change in *Arabidopsis thaliana* leaves lacking zeaxanthin belongs to a red-shifted sub-population of violaxanthin molecules formed during NPQ (23).

Transient absorption spectroscopy applied to purified LHCII in the aggregated, quenched state, has provided evidence that the pathway for energy dissipation may involve energy transfer from Chl *a* to the S_1 excited state of Lutein 1 (Lut1). The short lifetime of this Car S_1 state would ensure the efficient dissipation of the excitation energy into heat (9).

Because no consensus has yet been found to explain the molecular mechanism of qE, it is clear that further studies are needed to solve the present controversy. The quenching mechanism in LHCII has recently been investigated using a different approach, involving a newly developed system where the protein is immobilized in a gel matrix. Quenching could be induced in isolated LHCII trimers without protein aggregation, indicating that aggregation *per se* is not the cause of excitation energy quenching, thus supporting the conclusion that quenching is rather due to a protein conformational change (24). Direct and formal evidence of such a conformational change was provided by resonance Raman spectroscopy. This method revealed perturbation in the environments of Neo and Chl *b*, two chromophores that are not directly involved in the process of energy quenching (9, 18, 25). If the Lut1 molecule is indeed directly involved in the quenching mechanism one would predict that a conformational change in LHCII would modify its structure, thereby tuning its electronic properties and/or its interactions with nearby pigments. In this work, we address the reorganization of the Lut1 binding domain upon induction of quenching in LHCII using resonance Raman spectroscopy and discuss the mechanistic implications for NPQ.

EXPERIMENTAL PROCEDURES

LHCII Isolation—LHCII from wild-type (WT) *Arabidopsis* and the *npq2* mutant was isolated from unstacked thylakoid membranes according to the method described by Ruban *et al.* (26), with the exception that *n*-dodecyl α-D-maltoside was used rather than *n*-dodecyl β-D-maltoside, at a final concentration of 20 mM. LHCII was desalted in a PD10 desalting column (GE Healthcare) with a buffer containing 20 mM HEPES (pH 7.8) and 0.03% (w/v) *n*-dodecyl α/β-D-maltoside. Quenched LHCII was prepared by removal of detergent using SM-2 bioabsorbent beads (Bio-Rad), allowing for a 6-fold reduction in fluorescence yield as determined by a PAM-101 fluorometer (Heinz Walz). LHCII gel preparation and induction of quenching were performed as described previously (24).

Pigment Analysis—Pigment composition was determined by reverse-phase HPLC, using a LiChrospher 100 RP-18 column (Merck) and a Dionex Summit chromatography system, as described previously (27). The results of the analysis are summarized in Table 1. Chl concentration was determined according to the method of Porra *et al.* (28).

Resonance Raman Spectroscopy—Low temperature (77 K) resonance Raman spectra were obtained in a helium flow cryostat (Air Liquide) using a Jobin-Yvon U1000 Raman spectro-

photometer equipped with a liquid nitrogen-cooled charge-coupled device detector (Spectrum One, Jobin-Yvon) (29). Excitation was provided by a Coherent Argon laser (Innova 100; 488.0, 496.5, 501.7 nm) and a Liconix helium-cadmium laser (441.6 nm). The choice of these wavelengths was determined by the absorption maxima of the pigments derived from low temperature absorption spectra, as described by Ruban *et al.* (30).

Two-photon Spectroscopy—The details of this method have been described in Ref. 14. Briefly, a 1188-nm excitation is used for the two-photon excitation of Cars in LHCII, with careful rejection of visible light from the signal beam, to avoid one-photon excitation of Chls. This excitation was steered into a confocal setup and focused, and two-photon fluorescence was detected by an ultrafast photodiode connected to a lock-in amplifier (EG&G, Dumberry). For one-photon excitation of LHCII, a conventional Pulse Amplitude Modulation fluorometer (FMS1, Hansatech) (PAM) was integrated into the confocal setup, using a beam of 594 nm to excite LHCII Chls directly. Fluorescence was measured on the same spot for both two-photon and one-photon excitation, thus, allowing the determination of changes in electronic interaction between Cars and Chls in different quenched states. To avoid collection of the fluorescence more than once from the same spot of the LHCII gels, a homemade rotating device supporting the gels was used.

RESULTS

Evidence for Lut1 Changes in Quenched LHCII—As stated above, no Raman evidence of lutein structural changes in LHCII upon quenching has been reported up to now. However, selectivity between the different LHCII Cars cannot be fully achieved in resonance Raman due to their overlapping absorption bands (note that the absorption maxima of Lut1 and Neo are only 7 nm apart, at 495 and 488 nm, respectively; Ref. 30). Because the magnitude of any Raman changes seen is directly related to the extent of the Car structural change involved, the large Neo distortion occurring upon quenching could impair the observation of any lutein changes, if they are smaller. We therefore studied LHCII from the *npq2* mutant of *Arabidopsis* plants, which lack Neo (Table 1). Excitation at 488 nm favors contributions of Neo in WT LHCII (30). Using this excitation, spectra of the WT complexes display fingerprint bands of the 9-*cis* configuration of Neo molecules, at 1135, 1203, and 1215 cm^{-1} (Fig. 1, *black trace* (31). In spectra of *npq2* LHCII at the same excitation, these bands are missing (Fig. 1, *gray trace*; see also the WT − *npq2* difference spectrum, *dashed trace*).

In the ν_4 region of resonance Raman spectra, between 900 and 1000 cm^{-1}, bands arising from C-H out-of-plane wagging modes contribute to the spectrum. For strictly planar Car molecules, these modes are not coupled with the S_0-S_2 transition, and thus bands in this region of the spectrum are extremely weak. However, these bands may gain in intensity when the molecules are distorted around C-C bonds, so they constitute reliable markers of the Car configuration (29). In resonance Raman spectra of LHCII from *npq2* plants, bands at 956, 966, and 971 cm^{-1} clearly gain intensity (Fig. 2) when these complexes are quenched, and the change is most pronounced when 496.5-nm excitation was used (Fig. 2*B*). In the absence of Neo in these samples, this indicates that one lutein undergoes a small

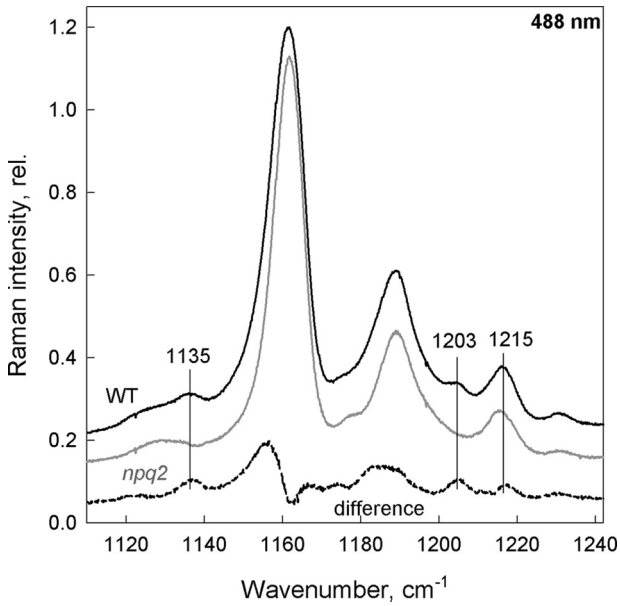

FIGURE 1. **ν_2 region of resonance Raman spectra obtained at 488.0 nm.** Isolated trimeric LHCII from WT (*black*), *npq2* (gray) *Arabidopsis* plants and the associated WT − *npq2* difference (*dashed*) highlighting the absence of *cis*-modes (*vertical lines*) in the *npq2* samples.

but significant change in configuration and that the lutein involved is the blue-absorbing one (495 nm), *i.e.* Lut1.

Do These Changes Exist in WT LHCII?—A change in the Lut1 configuration is thus observed upon quenching in LHCII purified from *npq2* plants. However, it could be argued that this change might only occur when Neo is not present, due to perturbation of the protein structure caused by an empty binding locus.

Lutein Changes in Aggregated WT LHCII—To test whether the changes in lutein configuration occur also when Neo is present, we repeated these experiments on aggregated LHCII isolated from WT *Arabidopsis* plants. Fig. 3*A* displays the aggregation-induced differences in Car spectra attributable to Neo, which peak at 488.0 nm excitation and still dominate the differential traces at redder excitations (496.5 and 501.7 nm). As discussed above, this is why it has been difficult to ascertain the presence of changes in lutein structure prior to this report. Nevertheless, as the Neo bands lose intensity at the higher excitation wavelengths, smaller additional bands are indeed seen in the differences (Fig. 3*A*) which may correspond to those observed in the absence of Neo (see Fig. 2). However, these features only represent minor contributions, and their exact frequencies are difficult to determine under the stronger Neo bands. Because the dominating bands from Neo are maximal at this Car absorption maximum, *i.e.* at 488.0 nm, while at longer wavelengths these contributions diminish but should not be shifted in frequency to any large extent, it is possible to extract the additional (non-Neo) bands by calculating double differences between the difference spectra. Thus, the traces $\Delta_{496.5} - \Delta_{488}$ and $\Delta_{496.5} - \Delta_{501.7}$, calculated with an arbitrary normalization factor designed to minimize the dominating Neo bands, give an approximation of the underlying spectral differences peaking at 496.5 nm. Surprisingly, the results are very similar, apart from a slight up-shift of the $\Delta_{496.5} - \Delta_{488}$ (*black trace*)

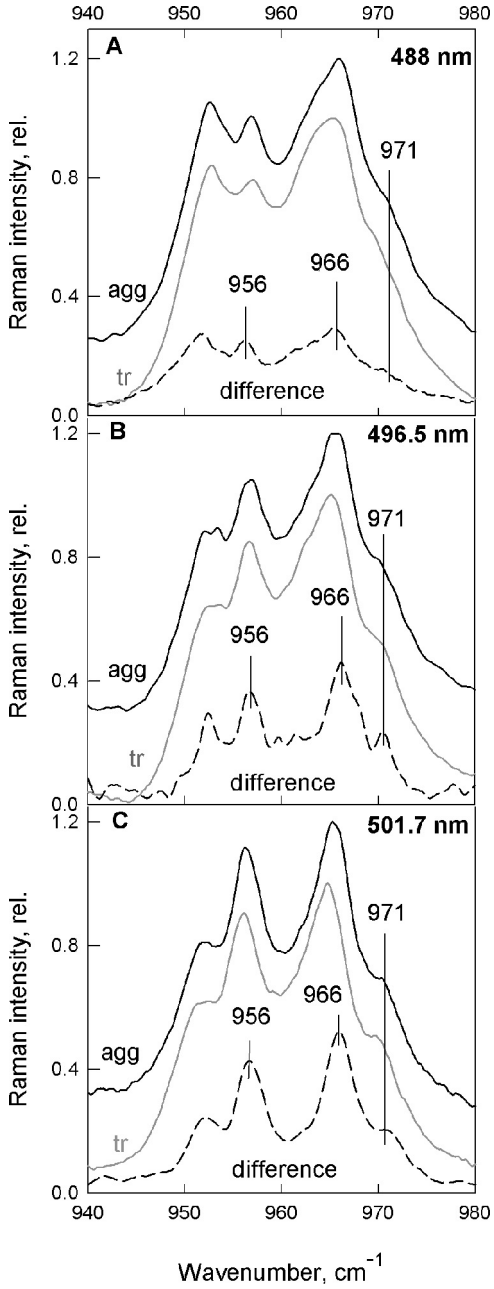

FIGURE 2. **ν_4 region of resonance Raman spectra recorded at 488.0, 496.5, and 501.7 nm (*A–C*, respectively).** Trimeric (*gray*), aggregated (*black*) LHCII isolated from *Arabidopsis npq2* plants and the associated difference spectra (aggregated − trimeric) are shown for each excitation wavelength (*dashed*; normalization at 1003 cm^{-1}).

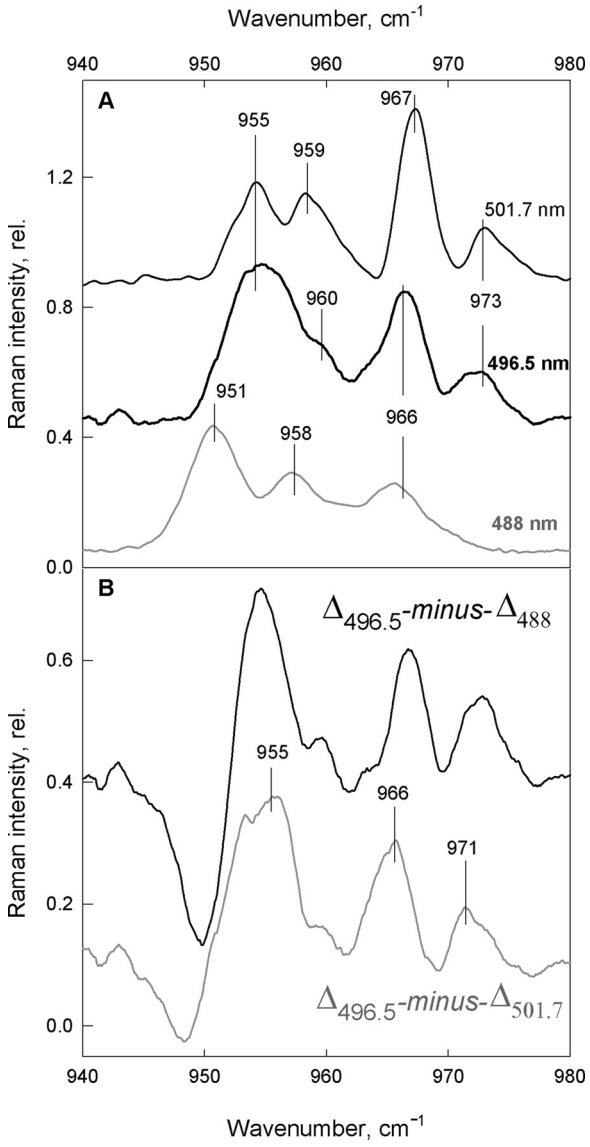

FIGURE 3. **Difference-associated (aggregated minus trimeric) resonance Raman spectra.** *A*, ν_4 region of WT LHCII obtained with 488 nm (*gray*), 496.5 nm (*thick black*), and 501.7 nm (*thin black*) excitation lines. *B*, double-difference spectra $\Delta_{496.5} - \Delta_{488}$ (*black*) and $\Delta_{496.5} - \Delta_{501.7}$ (*gray*) showing Lut1 changes (*vertical lines*) peaking at 496.5 nm (for details, see "Results").

with respect to $\Delta_{496.5} - \Delta_{501.7}$ (*gray trace*) (Fig. 3*B*). Both double-difference spectra show the same bands as present in the single-difference spectra for *npq2* samples, in the absence of Neo (*i.e.* 955, 966, and 971 cm^{-1}; see Fig. 2). This is a very good indication that we have successfully isolated the differential bands of Lut1, peaking at 496.5 nm ((0,0) transition of Lut1 is at 495 nm as in Ref. 30) and confirms the distortion of this pigment upon aggregation-induced quenching of LHCII.

Quenching in LHCII Gels—It has recently been shown that quenching can be produced in LHCII trimers in the absence of aggregation (24). This LHCII gel system has two advantages over aggregated LHCII for studying the quenching mechanism: the lack of aggregation results in samples of better optical quality because light scattering is almost entirely absent, and the samples can be quenched easily and to a greater extent. Thus, it should be possible to obtain better quality difference spectra for the observed changes in Lut1 even in the presence of Neo by using this new gel system. However, the structural changes associated with this aggregation-free quenching mechanism have not yet been characterized. It is therefore necessary to verify that the same structural mechanism is responsible for quenching in the gel system before using it to characterize further the structural changes involved.

Resonance Raman experiments were therefore performed on LHCII embedded in gels, at several excitations. 488.0 nm excitation favors Neo contributions, and, upon aggregation-induced quenching, or in LHCII crystals (33) (where LHCII are always quenched; Refs. 18, 47), a strong resonance Raman sig-

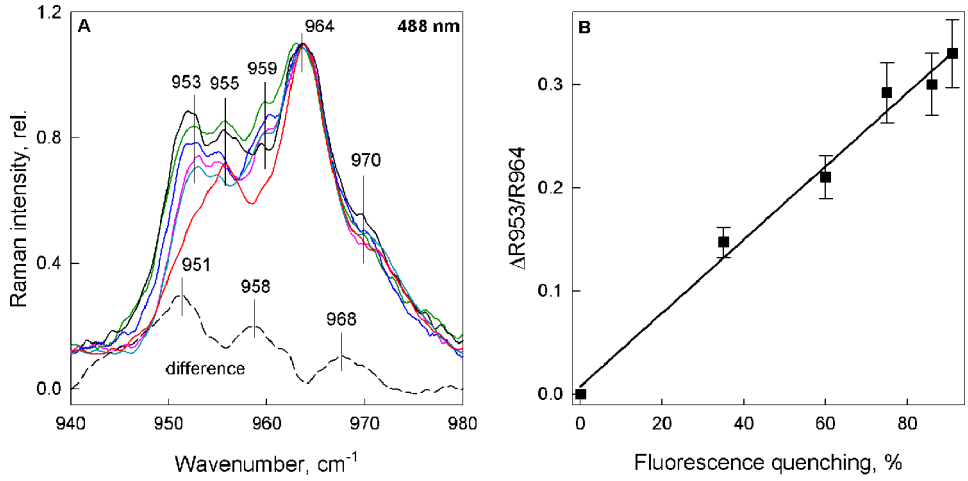

FIGURE 4. **ν_4 region of the resonance Raman spectra for Neo excitation (488.0 nm).** *A*, LHCII gels in the unquenched state (*red*) and with increasing levels of quenching (*cyan*, 35%; *magenta*, 60%; *blue*, 75%; *green*, 86%; *black*, 91%). Spectra were normalized at 964 cm^{-1}. The *dotted line* displays the difference spectrum quenched − unquenched for maximum quenching (91%), after normalization in the ν_3 region. *Vertical lines* indicate the vibrational modes discussed under "Results." *B*, relationship between the change in 953 cm^{-1} Raman intensity (relative to 964 cm^{-1} intensity) from *A* and the extent of fluorescence quenching, expressed as a percentage of fluorescence in the unquenched LHCII gel. The *error bars* in *B* are the calculated amplitude of noise on the spectrum obtained using Datamax GRAMS32 Galactic software (Instruments SA).

nal in the ν_4 is observed, indicating that Neo undergoes a change in configuration. Fig. 4*A* shows the same ν_4 region for 488.0 nm excitation of LHCII gels in different quenching states (see figure legend for details). The spectrum of the unquenched LHCII gel (*red trace*) shows two typical bands at 955 and 964 cm^{-1}, as observed previously for trimeric LHCII in solution (9, 18, 25). Upon induction of fluorescence quenching the enhancement of several vibrational modes is observed, the most prominent being the 953 cm^{-1} band. The increase in this vibrational mode relative to 964 cm^{-1} has previously been used to quantify the distortion of the Neo molecule, and this parameter was found to be linearly related to the quenching strength in aggregated LHCII as well as *in vivo* (9). For the quenched LHCII gels measured here, the same linear relationship is observed (Fig. 4*B*).

Comparison of the resonance Raman signal of LHCII trimers and aggregates at 441.6 nm excitation, which favors Chl *b* contributions, has shown that the formyl group of at least one Chl *b* (and possibly two) enters into a stronger interaction with its environment upon aggregation-induced quenching. This strong H bond was also observed in quenched LHCII in crystals (18). Again, the same changes are observed when quenching is induced in LHCII gels (Fig. 5). Upon quenching, a 1639 cm^{-1} band gains intensity, indicating the presence of strongly interacting formyl groups which, in unquenched samples, were free from interactions. The full width at half maximum of this additional band (6–7 cm^{-1}) represents a high degree of homogeneity in bonding strength for this new H bond in the quenched state, indicating an interaction that is tightly controlled by the protein (Raman bands of single populations are usually approximately 13 cm^{-1} full width at half maximum in biological samples) (25, 34). Note that this was again the case for aggregation-induced quenching and in quenched LHCII crystals (18, 25, 47).

Several studies have provided evidence that electronic interactions between Car S_1 and Chls may play a key role in the dissipation of excess excitation energy (3, 9, 35). To test the involvement of the Car S_1 state in the quenching process in

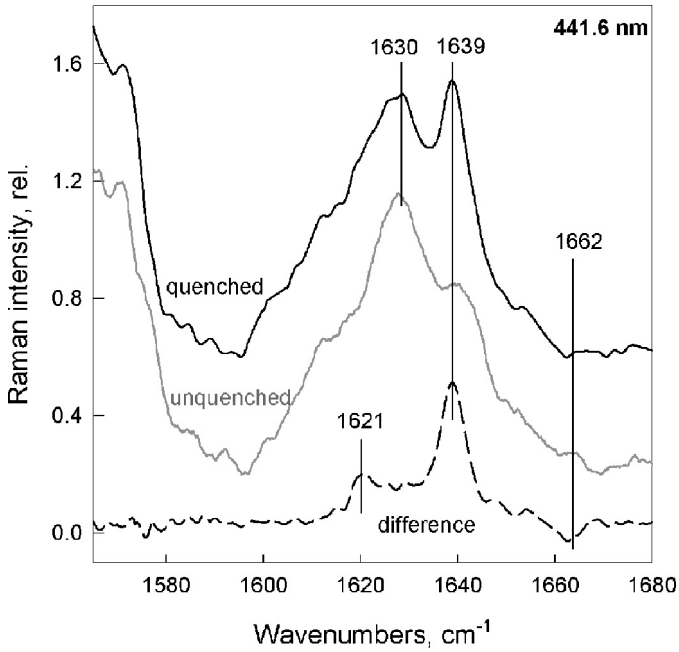

FIGURE 5. **Chl *b* resonance Raman spectra of the unquenched (*gray*) and quenched (*black*) LHCII gels at 441.6 nm excitation.** The difference spectrum (quenched − unquenched; *dashed trace*) shows the typical, narrow 1639 cm^{-1} band (full width at half maximum = 6–7 cm^{-1}) assigned to H bond formation (18, 20). Quenching in gels was 91%.

LHCII gels, two-photon excitation spectroscopy was performed, similar to that reported in Ref. 14 on LHCII trimers, aggregates, and whole plants. According to optical selection rules, direct electronic transition from S_0 to S_1 is forbidden, but this transition is, however, two-photon allowed (36, 37), and energy transfer from the S_1 state of carotenoid to Chl can thus be probed by Chl fluorescence upon two-photon excitation. Comparing two-photon Chl fluorescence with fluorescence upon direct one-photon Chl excitation allows quantification of the electronic interaction between Cars and Chls (38). In isolated LHCII, as well as in intact plants, this interaction corre-

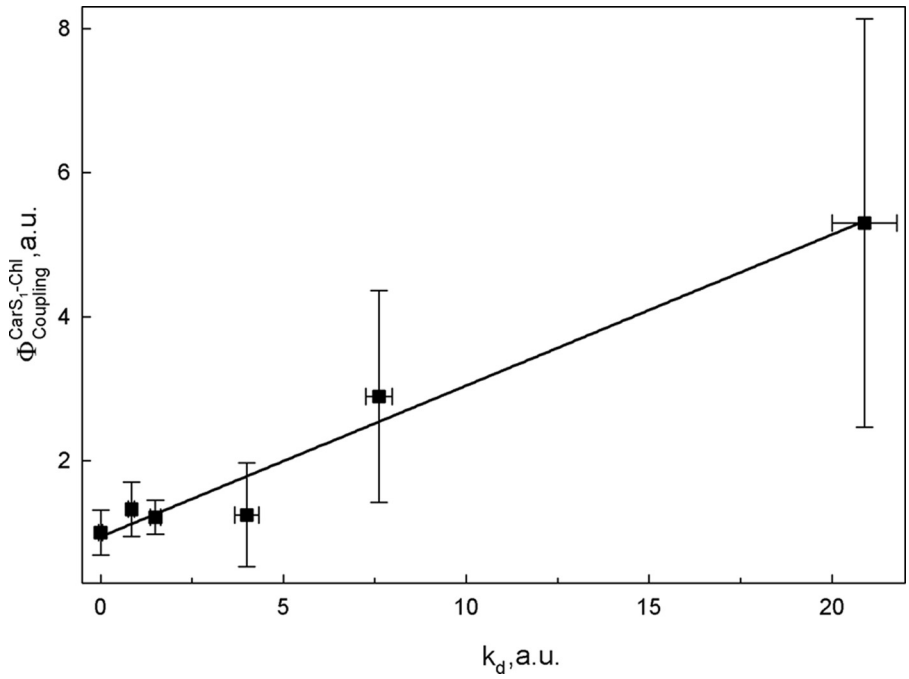

FIGURE 6. **Correlation of $\phi^{Car\ S_1}_{Coupling}$—Chl with fluorescence quenching (presented as k_d), for quenched LHCII in the gel system.** Fluorescence quenching was induced as in Ilioaia *et al.* (24). Samples were 10, 27, 40, 60, and 78% quenched compared with the unquenched LHCII gel (0%). This corresponds to 0.11, 0.37, 0.67, 1.5, and 3.55 k_d values, respectively. *Error bars*, S.E.

lates linearly with fluorescence quenching (14, 39, 40). In Fig. 6 this correlation is shown for LHCII gels at various different quenching levels (see legend). Here, k_d was calculated from the fluorescence measured with a PAM fluorometer (as described under "Experimental Procedures"), where F_{unq} and F_q are fluorescence intensities of unquenched and quenched samples, respectively.

$$k_d = \frac{F_{unq}}{F_q} - 1 \qquad \text{(Eq. 1)}$$

This linear correlation confirms that quenching in LHCII in the absence of aggregation shares the same properties and that it thus involves the same mechanism(s) as for aggregation-induced quenching.

We have thus established that quenching in the LHCII gel system has all of the same spectral characteristics as that in aggregation-induced quenching, and so we can now use this system to investigate the changes in Lut1 structure further. The ν_4 region of resonance Raman spectra obtained with excitation at 496.5 and 501.7 nm of unquenched and quenched LHCII complexes in gels are displayed in Fig. 7, *B* and *C*, along with their associated quenched − unquenched differences. The 488 nm spectra are also plotted for comparison, together with the associated difference spectrum (Fig. 7*A*, taken from Fig. 4). The fingerprint of Neo distortion is again present at 488 nm excitation (Fig. 7*A*) and is still strong at 496.5 nm (Fig. 7*B*). However, at 501.7 nm (Fig. 7*C*) this Neo contribution is reduced significantly, and as a result the emergence of the three new bands at 955, 966, and 973 cm^{-1} is clearly seen. Note that at 496.5 nm, these bands can also be observed, on top of the dominant Neo contributions (951, 958, and 968 cm^{-1}) indicated by arrows. These new bands, which correspond exactly to those observed in the LHCII aggregation experiments (though less clearly in the presence of Neo), must reflect the distortion of the same Car, *i.e.* Lut1 (Lut 620 from the crystal structure of Liu *et al.;* Ref. 33).

DISCUSSION

In this study we have shown that, along with the known changes in pigment configuration that accompany fluorescence quenching in aggregates of LHCII complexes (involving Neo, Chl *a*, and Chl *b*) (9, 18, 25), there is also a change in the Lut1 binding domain. Lut1 undergoes a distortion during the transition of LHCII into the quenched state. We also show here that LHCII quenching in the absence of protein aggregation, in a recently developed gel system (24), displays all of the spectral signatures observed previously in LHCII aggregates. This indicates that fluorescence quenching in the LHCII gels occurs by the same mechanism(s) as aggregation-induced quenching. The absence of scattering artifacts in this new model system results in spectra of much higher quality, allowing us to confirm the small but significant changes in Raman signature of the Lut1 molecule.

The structural change in Lut1 may reflect its specific activation by the LHCII conformational change as the excitation energy quencher, either by increasing Chl *a*–Lut1 coupling interactions (14, 41) or by mediating more efficient energy transfer from Chl *a* to the Lut1 S_1 state (9), or both. Alternatively, the twisting of Lut1 observed here could alter its excited state properties influencing the likelihood of energy transfer between Chl *a* and the Lut1 S_1 state (42). Indeed, spectral changes in the terminal emitter chlorophylls, *a*610, *a*611, and *a*612, that lie in van-der-Waals contact with Lut1 (33), have also been observed during quenching in isolated LHCII and *in vivo*

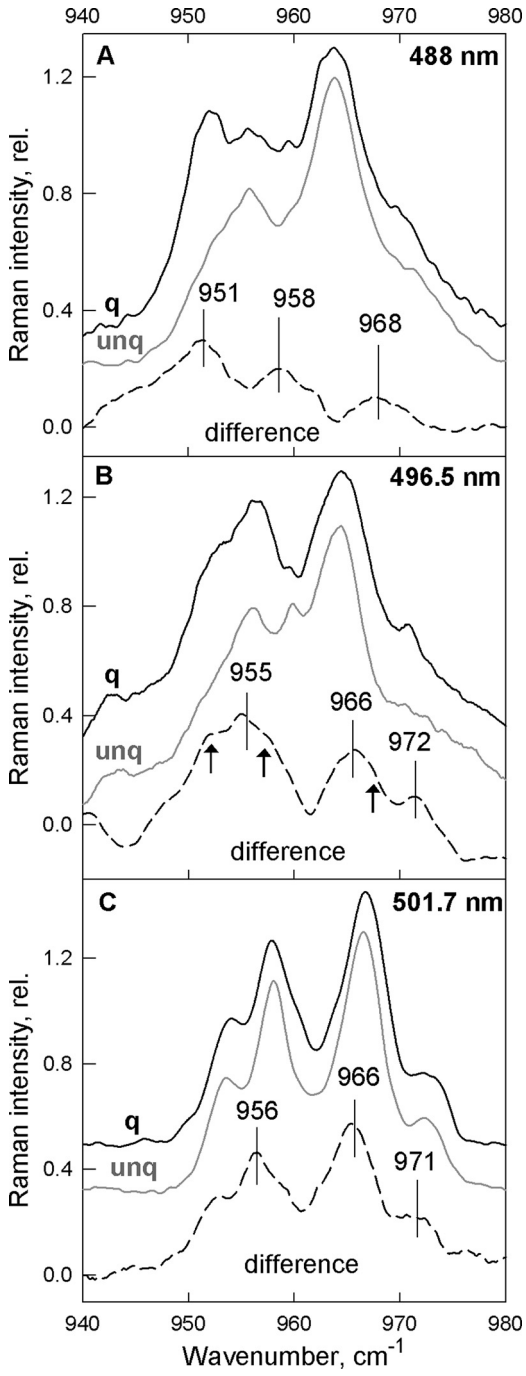

FIGURE 7. **ν_4 region of the resonance Raman spectra recorded at 488.0, 496.5, and 501.7 nm (*A–C*, respectively) for LHCII gels.** Unquenched (*gray*) and quenched (*black*) LHCII gels are presented together with the difference-associated spectra (quenched − unquenched), calculated for each excitation (*dashed*), showing the presence of the new vibrational modes. Arrows in *B* indicate the Neo vibrations present as shoulders at 496.5-nm excitation.

(43), providing further evidence of a change in this domain. The two-photon excitation spectroscopy data reported here and our preliminary results from transient absorption spectroscopy on quenched LHCII gels upon selective Chl *a* excitation lend support to the view that a Car S_1 excited state is transiently populated from the excited Chl in a way similar to that observed in artificial photosynthetic antennas (44) and aggregated LHCII (9).

Early work on xanthophyll biosynthetic mutants of *Arabidopsis* lacking lutein showed that the absence of this pigment reduced NPQ by ~30% (45). In these lutein-deficient plants, lutein is replaced at the Lut1 and Lut2 sites by a mixture of violaxanthin, antheraxanthin, and zeaxanthin that, unlike the "normal" xanthophyll cycle pigments in the WT were not available for (de-)epoxidation (45, 46). Lokstein *et al.* thus argued that, because zeaxanthin was known to be important for NPQ, the lack of any increase in the capacity for NPQ in these mutants indicated that the xanthophylls in the Lut1 and Lut2 sites are not directly involved in quenching (46). They postulated that the decrease in NPQ capacity in the lutein mutants was in fact due to the modified structure of LHCII (46). However, this interpretation neglects the fact that such structural changes may negatively affect the interactions between the xanthophyll bound at the Lut1 site and the terminal emitter chlorophylls. Thus, zeaxanthin may actually be a weaker quencher than lutein at this site, explaining the reduction in NPQ in the lutein-deficient plants.

Alternatively, it is possible that the structural changes in Lut1, and indeed those previously reported in Neo (9, 18, 25), Chl *b* (18, 25), zeaxanthin (21) and violaxanthin (23) may simply reflect the conformational change in the LHCII that engage Chl-Chl quenching interactions as suggested by Holzwarth and co-workers (15, 16). Indeed, in such an interpretation the disrupted LHCII structure in mutants lacking lutein could directly affect the Chl-Chl interactions resulting in the observed reduction in NPQ.

Irrespective of whether xanthophylls are directly involved in the quenching mechanism, the observed changes in Lut1 contribute to our growing knowledge of the microscopic alterations in LHCII conformation that occur upon transition to the quenched state. Our growing insight into the finer details of these changes will allow us to form a more complete picture of how and why changes in LHCII conformation result in quenching.

REFERENCES

1. Horton, P., Ruban, A. V., and Walters, R. G. (1996) *Annu. Rev. Plant Physiol. Plant Mol. Biol.* **47,** 655–684
2. Niyogi, K. K. (1999) *Annu. Rev. Plant Physiol. Plant Mol. Biol.* **50,** 333–359
3. Holt, N. E., Fleming, G. R., and Niyogi, K. K. (2004) *Biochemistry* **43,** 8281–8289
4. Müller, P., Li, X. P., and Niyogi, K. K. (2001) *Plant Physiol.* **125,** 1558–1566
5. Briantais, J. M., Vernotte, C., Picaud, M., and Krause, G. H. (1979) *Biochim. Biophys. Acta* **548,** 128–138
6. Demmig-Adams, B., Adams, W. W., Heber, U., Neimanis, S., Winter, K., Krüger, A., Czygan, F. C., Bilger, W., and Björkman, O. (1990) *Plant Physiol.* **92,** 293–301
7. Li, X. P., Björkman, O., Shih, C., Grossman, A. R., Rosenquist, M., Jansson, S., and Niyogi, K. K. (2000) *Nature* **403,** 391–395
8. Li, X. P., Gilmore, A. M., Caffarri, S., Bassi, R., Golan, T., Kramer, D., and Niyogi, K. K. (2004) *J. Biol. Chem.* **279,** 22866–22874
9. Ruban, A. V., Berera, R., Ilioaia, C., van Stokkum, I. H., Kennis, J. T., Pascal, A. A., van Amerongen, H., Robert, B., Horton, P., and van Grondelle, R. (2007) *Nature* **450,** 575–578
10. Holt, N. E., Zigmantas, D., Valkunas, L., Li, X. P., Niyogi, K. K., and Fleming, G. R. (2005) *Science* **307,** 433–436
11. Ahn, T. K., Avenson, T. J., Ballottari, M., Cheng, Y. C., Niyogi, K. K., Bassi, R., and Fleming, G. R. (2008) *Science* **320,** 794–797
12. Holzwarth, A. R., Miloslavina, Y., Nilkens, M., and Jahns, P. (2009) *Chem. Phys. Lett.* **483,** 262–267

13. Avenson, T. J., Ahn, T. K., Zigmantas, D., Niyogi, K. K., Li, Z., Ballottari, M., Bassi, R., and Fleming, G. R. (2008) *J. Biol. Chem.* **283,** 3550–3558
14. Bode, S., Quentmeier, C. C., Liao, P. N., Hafi, N., Barros, T., Wilk, L., Bittner, F., and Walla, P. J. (2009) *Proc. Natl. Acad. Sci. U.S.A.* **106,** 12311–12316
15. Müller, M. G., Lambrev, P., Reus, M., Wientjes, E., Croce, R., and Holzwarth, A. R. (2010) *Chem. Phys. Chem.* **11,** 1289–1296
16. Miloslavina, Y., Wehner, A., Lambrev, P. H., Wientjes, E., Reus, M., Garab, G., Croce, R., and Holzwarth, A. R. (2008) *FEBS Lett.* **582,** 3625–3631
17. Horton, P., Wentworth, M., and Ruban, A. V. (2005) *FEBS Lett.* **579,** 4201–4206
18. Pascal, A. A., Liu, Z., Broess, K., van Oort, B., van Amerongen, H., Wang, C., Horton, P., Robert, B., Chang, W., and Ruban, A. V. (2005) *Nature* **436,** 134–137
19. Krüger, T. P., Novoderezhkin, V. I., Ilioaia, C., and van Grondelle, R. (2010) *Biophys. J.* **98,** 3093–3101
20. Johnson, M. P., Pérez-Bueno, M. L., Zia, A., Horton, P., and Ruban, A. V. (2009) *Plant Physiol.* **149,** 1061–1075
21. Ruban, A. V., Pascal, A. A., Robert, B., and Horton, P. (2002) *J. Biol. Chem.* **277,** 7785–7789
22. Noctor, G., Ruban, A. V., and Horton, P. (1993) *Biochim. Biophys. Acta* **1183,** 339–344
23. Ilioaia, C., Johnson, M. P., Duffy, C. D., Pascal, A. A., van Grondelle, R., Robert, B., and Ruban, A. V. (2011) *J. Biol. Chem.* **286,** 91–98
24. Ilioaia, C., Johnson, M. P., Horton, P., and Ruban, A. V. (2008) *J. Biol. Chem.* **283,** 29505–29512
25. Ruban, A. V., Horton, P., and Robert, B. (1995) *Biochemistry* **34,** 2333–2337
26. Ruban, A. V., Lee, P. J., Wentworth, M., Young, A. J., and Horton, P. (1999) *J. Biol. Chem.* **274,** 10458–10465
27. Johnson, M. P., Havaux, M., Triantaphylidès, C., Ksas, B., Pascal, A. A., Robert, B., Davison, P. A., Ruban, A. V., and Horton, P. (2007) *J. Biol. Chem.* **282,** 22605–22618
28. Porra, R. J., Thompson, W. A., and Kriedemann, P. E. (1989) *Biochim. Biophys. Acta* **975,** 384–394
29. Robert, B., and Lutz, M. (1986) *Biochemistry* **25,** 2303–2309
30. Ruban, A. V., Pascal, A. A., and Robert, B. (2000) *FEBS Lett.* **477,** 181–185
31. Ruban, A. V., Pascal, A. A., Robert, B., and Horton, P. (2001) *J. Biol. Chem.* **276,** 24862–24870
32. Robert, B., Horton, P., Pascal, A. A., and Ruban, A. V. (2004) *Trends Plant Sci.* **9,** 385–390
33. Liu, Z., Yan, H., Wang, K., Kuang, T., Zhang, J., Gui, L., An, X., and Chang, W. (2004) *Nature* **428,** 287–292
34. Lutz, M. (1984) in *Advances in IR and Raman Spectroscopy* (Clark, R. J. H., and Hetser, R. E., eds) pp. 211–300, John Wiley and Sons Inc., New York
35. Frank, H. A., Bautista, J. A., Josue, J. S., and Young, A. J. (2000) *Biochemistry* **39,** 2831–2837
36. Wehling, A., and Walla, P. J. (2005) *J. Phys. Chem. B* **109,** 24510–24516
37. Hilbert, M., Wehling, A., Schlodder, E., and Walla, P. J. (2004) *J. Phys. Chem. B* **108,** 13022–13030
38. Frähmcke, J. S., and Walla, P. J. (2006) *Chem. Phys. Lett.* **430,** 397–403
39. Liao, P.-N., Bode, S., Wilk, L., Hafi, N., and Walla, P. J. (2010) *Chem. Phys.* **373,** 50–55
40. Bode, S., Quentmeier, C. C., Liao, P.-N., Barros, T., and Walla, P. J. (2008) *Chem. Phys. Lett.* **450,** 379–385
41. van Amerongen, H., and van Grondelle, R. (2001) *J. Phys. Chem. B* **105,** 604–617
42. Dreuw, A. (2006) *J. Phys. Chem. A* **110,** 4592–4599
43. Johnson, M. P., and Ruban, A. V. (2009) *J. Biol. Chem.* **284,** 23592–23601
44. Berera, R., Herrero, C., van Stokkum, I. H., Vengris, M., Kodis, G., Palacios, R. E., van Amerongen, H., van Grondelle, R., Gust, D., Moore, T. A., Moore, A. L., and Kennis, J. T. (2006) *Proc. Natl. Acad. Sci. U.S.A.* **103,** 5343–5348
45. Pogson, B. J., Niyogi, K. K., Björkman, O., and DellaPenna, D. (1998) *Proc. Natl. Acad. Sci. U.S.A.* **95,** 13324–13329
46. Lokstein, H., Tian, L., Polle, J. E., and DellaPenna, D. (2002) *Biochim. Biophys. Acta* **1553,** 309–319
47. van Oort, B., Maréchal, A., Ruban, A. V., Robert, B., Pascal, A. A., de Ruiter, N., van Grondelle, R., and van Amerongen, H. (2011) *Phys. Chem. Chem. Phys.*, in press